CHARACTERIZATION OF BIOMATERIALS USING MAGNETIC RESONANCE ELASTOGRAPHY

J. A. Smith, R. Muthupillai, P. J. Rossman,
T. C. Hulshizer, J. F. Greenleaf, R. L. Ehman
Department of Diagnostic Radiology
Mayo Clinic and Foundation
Rochester, MN 55905

INTRODUCTION

Many diseases are known to change the mechanical properties of tissue. For example, cancerous lesions tend to feel rigid when touched and infectious lesions tend to feel soft when compared to the surrounding tissue. This is why palpation is a useful diagnostic procedure.

During many abdominal operations, palpation is used to assess internal organs such as the liver. It is not uncommon for surgeons at the time of abdominal surgery to discover by touch liver tumors that were undetected in preoperative imaging by computed tomography, magnetic resonance imaging or ultrasonography. None of the imaging modalities are capable of assessing the types of mechanical properties elicited by palpation. These observations provide motivation for seeking a medical imaging technology that can depict the mechanical properties of tissue and provide the hypothesis of this research. Our research hypothesis is that "palpation by imaging" will be a useful diagnostic tool for characterizing diseases. This may provide a way to noninvasively "palpate" regions of the body which are inaccessible to the physician's hand and might permit the identification of small tumors before they are large enough to detect by touch.

Mechanical properties offer a wider scale for characterizing tissues than normal medical imaging modalities. The elastic moduli of soft tissue vary by as much as four orders of magnitude [1]. Changes in the mechanical properties of tissue due to disease can also be significant. Tumors found in the breast illustrate changes in the mechanical properties between normal tissue, benign tumors and malignant tumors. For instance, a breast tumor can have an elastic modulus which is almost two orders of magnitude greater than normal breast tissue [2].

Since these measurable changes in tissue properties are potentially useful as a diagnostic tool, methods are being sought to quantify the properties of tissue. These methods can be grouped into three types: Static, Quasi-static and Dynamic.

Review of Progress in Quantitative Nondestructive Evaluation, Vol. 16
Edited by D.O. Thompson and D.E. Chimenti, Plenum Press, New York, 1997

The static methods [3] are not useful for clinical applications since tissue samples must be excised and placed in a testing machine. The quasi-static methods [4], correlate speckle from an unloaded specimen and a loaded specimen in B-mode ultrasonic images. These methods are sensitive to specimen geometry and boundary conditions. The dynamic methods [5,6] use Doppler ultrasound to monitor acoustic shear waves in tissue. The propagation characteristics of the shear waves are a measure of the tissue's mechanical properties. This method is limited to monitoring tissues which have an acoustic window and are in the line of sight of the ultrasonic transducer. Also, only motion along the axis of the ultrasonic beam can be detected.

The dynamic method being discussed in this paper is Magnetic Resonance Elastography (MRE) [7,8]. MRE combines the benefits of acoustic shear waves and of Magnetic Resonance Imaging (MRI). The acoustic shear waves remotely "palpate" tissue while being imaged by MRI. MRI has high imaging resolution and is used to measure the displacements caused by shear waves. The measurable displacement magnitudes are on the order of 100 nm or greater along any axis.

MRE uses a standard MRI scanner at 1.5T to generate two dimensional displacement images of cyclic shear waves propagating in tissue. Shear waves between 10 Hz - 1.1 kHz are used to characterize tissue because shear wavelengths are much shorter than longitudinal wavelengths at these frequencies. A tissue with high rigidity will propagate a shear wave faster than a softer tissue for a given density.

Full field velocity and attenuation measurements can be made in tissue by imaging the displacements caused by propagating shear waves. The measured values for shear wave velocity and attenuation depends on the viscoelastic properties of the tissue and on the frequency of the propagating wave. Thus a tissue can be characterized by velocity and attenuation measurements at different acoustic frequencies. The objective of this research is to use Magnetic Resonance Elastography to measure the viscoelastic properties of velocity and attenuation as a function of shear wave frequency in Bovine Gel.

In the next section, a basic review of physics for Magnetic Resonance and MRE is given. Then the MRE imaging system is discussed. This will be followed by the experimental methods used to obtain the dispersion measurements and the resulting dispersion curves. A discussion of the results from the dispersion measurements are presented next. Finally, the conclusions summarizing the results are given.

REVIEW OF MAGNETIC RESONANCE AND MRE PHYSICS

The magnetic resonance phenomena can be studied by observing the behavior of nuclear spins, usually hydrogen atoms, in a magnetic field, B_0, as shown in Figure 1. This set of spins has a resonance frequency, ω_0, given by the Larmor equation [9]. Gamma, the gyromagnetic ratio, is a property of the nucleus. An RF electromagnetic pulse, whose frequency content contains a frequency component at ω_0, is then transmitted. This RF pulse causes the spins to precess around the static magnetic field at the Larmor frequency. While the spins are precessing, a RF signal, also at the Larmor frequency, is induced in a receiver coil [9]. A heterodyne interferometer can be constructed from the known reference frequency (Larmor Frequency), and the measurable RF signal which should be near the Larmor Frequency.

The working principle behind MRE is very similar to heterodyne interferometry [7, 8]. The spins are placed in a magnetic field gradient to linearly change the precessional frequency of the spins with displacement as shown in Figure 2. When the spins are stationary, the received RF signal is at the reference Larmor frequency for the static B_0 field and there is no progression of phase between the two frequencies. When the spins are displaced from their mean position, the Larmor frequency changes and there is a progression of phase between the reference frequency and the RF signal. When the motion is cyclic in a static gradient field, the phase progression caused by positive displacements is canceled by phase regression caused by negative displacements. Thus over one period of the displacement cycle, there would be no net phase change between the reference frequency and the RF signal. To keep accumulating phase differences, the field gradient can be switched in polarity at the same frequency of the cyclic displacements as discussed in the next section.

MRE IMAGING SYSTEM

MRE uses a conventional MRI system with a sequence of RF pulses and magnetic field gradients to encode the spatial positions of hydrogen nuclei (spins) [7, 8] and reconstructs tomographic images using a Fourier transformation algorithm. The timing of the RF pulses, and magnetic field gradients (frequency encode, phase encode, slice select) [9], are shown schematically in Figure 3. In addition to the imaging gradients, a motion sensitizing gradient, which is switched in polarity at the same frequency as the mechanical excitation, is superimposed in the direction of motion measurement for the spins. The synchronous motion-sensitizing gradient can be applied to any magnetic field gradient axis or any combination of axes as indicated by the white boxes in the timing diagrams. Thus, the motion sensitizing gradient can be applied along any arbitrary axis to measure motion in any direction. The cyclic displacements of the spins in the presence of these motion-sensitizing gradients will cause a measurable phase shift in the received magnetic resonance signal.

By progressively varying the phase offset, θ, between the motion sensitizing gradients and the mechanical excitation, it is possible to obtain snapshots of the propagating acoustic wavefront as a function of time. One such snapshot is shown in the right portion of Figure 3. This is an actual phase difference image of a propagating shear wave in a gel phantom. This phase image is similar to an image that could be obtained by pulsed holographic interferometry and it contains similar displacement information.

The shear waves in the gel are generated by a mechanism similar to a voice coil actuator found in a loudspeaker. A wave generator, which is synchronized to the motion-sensitizing gradient, produces an alternating current in the actuator coil. In the presence of the static magnetic filed of the MRI scanner, the current in the actuator coil causes the contact plate which is connected to coil by an armature to move about the pivot point. The contact plate is a 9 x 9 mm "aperture" which produces plane wave fronts as shown in the MRE phase image.

The measured phase shifts are proportional to the scalar product of the displacement vector, the motion-sensitizing gradient vector, and to the number and the period of the

cyclic motion-sensitizing gradients as given by Equation 1 [7, 8]. Thus sensitivity to small amplitude cyclic motion can be increased by accumulating phase shifts over multiple cycles of the mechanical excitation and the motion-sensitizing gradient waveform. From the measured phase shift in each volume element, it is possible to measure the amplitude of displacement in from the reconstructed image.

$$\phi(\mathbf{r},\theta) = \frac{2\gamma NT(\mathbf{G} \bullet \mathbf{u})}{\pi} \sin(\mathbf{k} \bullet \mathbf{r} + \theta) \tag{1}$$

where:

ϕ	Phase shift
$\mathbf{r}$	Mean position of the spins
θ	Initial phase offset
γ	Gyromagnetic ratio which is characteristic of the nucleus
N	Number of gradient cycles
T	Period of the mechanical excitation
$\mathbf{G}$	Magnetic-field gradient vector
$\mathbf{u}$	Displacement vector of the spins
$\mathbf{k}$	Wave vector of the acoustic shear wave

For the all of the data presented in this paper, the imaging acquisition parameters for the MRI scanner are the following. The 256 x 256 pixel image has a field of view 14 cm which corresponds to an axial pixel size of 0.55 mm. The horizontal axis of the phase image is frequency encoded while the vertical axis is phase encoded [9]. The thickness of the axial slice is set at 5 mm. An echo time (TE) of 18 ms and a repetition time (TR) of 175 ms are used. TE is the amount of time between the RF pulse and the resulting Magnetic Resonance signal. TR is the amount of time to complete one imaging sequence of RF pulses and magnetic field gradients and start a new sequence. Each image frame takes 90 s to acquire. The amplitude of the Magnetic Field Gradient is set at 1.1 Gauss/cm.

METHODS

The objective of this research is to use MRE to measure the viscoelastic material properties of velocity and attenuation dispersion in Bovine Gel. To do this, a vertical line scan from the phase image of a propagating shear wave is used to fit a damped cosine, Equation 2. The fit is a five parameter non-linear best fit in a least squares manner to the line scan data. Signal averaging over 60 frequency encoded columns and bandpass filtering are used to obtain better estimates of the five parameters. The five parameters to be solved for are the following: u_0 is the amplitude of the displacement; α is the attenuation coefficient; λ is the wavelength; ψ is the phase offset; and k is a constant offset. The wavelength and attenuation coefficient are the parameters of interest at this time. Shear wave phase velocity, c_p, is proportional to the wavelength as shown in Equation 3.

$$u(t) = u_0 \exp(-\alpha r) \cdot \cos\left(\frac{2\pi}{\lambda} r - \omega t + \psi\right) + k \tag{2}$$

$$c_p = f \cdot \lambda \tag{3}$$

Plane wavefronts, as demonstrated by the phase image in Figure 3, are used to reduce the effects of geometric attenuation and to allow for more columns to be used in obtaining a better average of the line scans. Eight images with different phase offsets are used to determine eight pairs of wavelength and attenuation coefficients. The averages and standard of deviation for the eight pairs of data are reported.

Dispersion measurements at five frequencies are used: 100, 200, 300, 400, 500 Hz. These measurements are limited by the wavelength of the shear waves (>3.5 cm) below 100 Hz. The upper frequency measurements are limited by mechanical coupling efficiency, material attenuation, and displacement resolution above 500 Hz.

Five different concentrations of Bovine Gel are characterized by the dispersion measurements. The concentrations tested are the following: 10, 12, 14, 16, 18% by weight of water. It is assumed that the higher Gel concentrations have a higher rigidity and propagate the shear waves at faster phase velocities [10]. At concentrations below 10%, there is large attenuation of the shear wave. At concentrations above 18%, the gel is difficult to dissolve in the water. The Gel phantoms have a cure time of approximately 20 hrs unless otherwise noted.

RESULTS AND DISCUSSION

Figure 4 shows the velocity and attenuation dispersion graphs for the 10 and 16% Gels. There are no statistical differences between the 10, 12, and 14% Gels. The 18% Gel has significantly higher phase velocity and significantly lower attenuation. Therefore, for clarity, the 12, 14 and 18% gels are not shown in these graphs. Due to the increased rigidity of the 16 % Gel, the resulting shear displacements are less and this significantly decreased the signal to noise ratio of the measured phase velocities. This increased level of noise can be seen in the phase velocity plots by the increase in length of the error bars when compared to the 10% Gel data. Because of the increased level of noise, data were not collected at 500 Hz in the 16% Gel.

From Figure 4, two general trends can be noted. As the attenuation increases in the gel, the phase velocity tends to increase for both concentrations. As the relative attenuation increases between the concentrations at a single frequency, the difference in their phase velocities tend to increase. Figure 4 more clearly emphasizes these features.

Figure 5 shows the dispersion curves for 18% Gel with two different curing times. The 52 hour cure gel has the smallest amount of attenuation and almost no velocity dispersion. It behaves almost as a perfectly elastic medium. As the attenuation increases in the Gel with a 23 Hr cure, the phase velocity tends to increase.

From the data presented in Figures 4 and 5, the following results have been obtained. The velocity and attenuation resolutions are on the order of 0.1 m/s and 0.4 /cm. Velocity is nonlinear with respect to Gel composition and velocity increases with respect to concentration and cure time. Velocity magnitude and dispersion increases with attenuation which is consistent with the Voight viscoelastic model [11]. Also, Gel cure time plays an important role in determining the dispersion characteristics of the Gel phantom. Velocity measurements are more sensitive than attenuation to changes in Gel composition and cure time.

CONCLUSIONS

Magnetic Resonance Elastography has been demonstrated to measure velocity and attenuation in Gel phantoms with deviations from the mean on the order of 8% and 26% percent respectively. These precisions are sufficient to characterize velocity and attenuation dispersion caused by the viscoelastic properties of bovine Gel. In addition to these experimental conclusions, MRE has the following general conclusions. MRE does not require known boundary conditions to be effective, and it can measure displacements along an arbitrary axis to obtain three-dimensional displacement fields. Since MRE is a form of MRI, any soft tissue can be imaged even if surrounded by bone or air spaces. These characteristics of Magnetic Resonance Elastography have a high probability of making MRE an effective tool for noninvasive characterization of in vivo tissue.

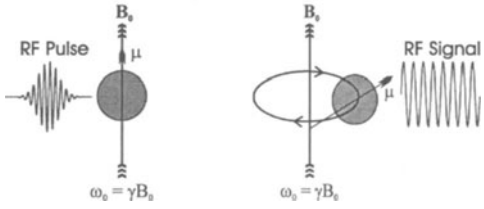

Figure 1. Illustration of a collection of nuclear spins precessing in a magnetic field.

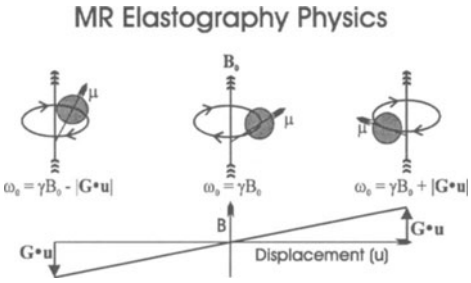

Figure 2. Spins have a phase progression when displaced in a magnetic field gradient.

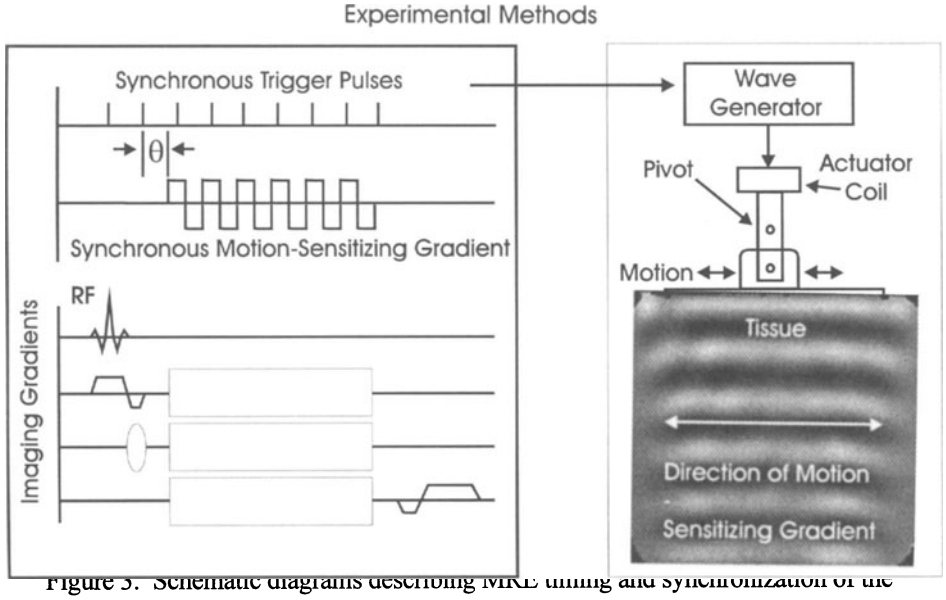

Figure 3. Schematic diagrams describing MRE timing and synchronization of the mechanical actuator.

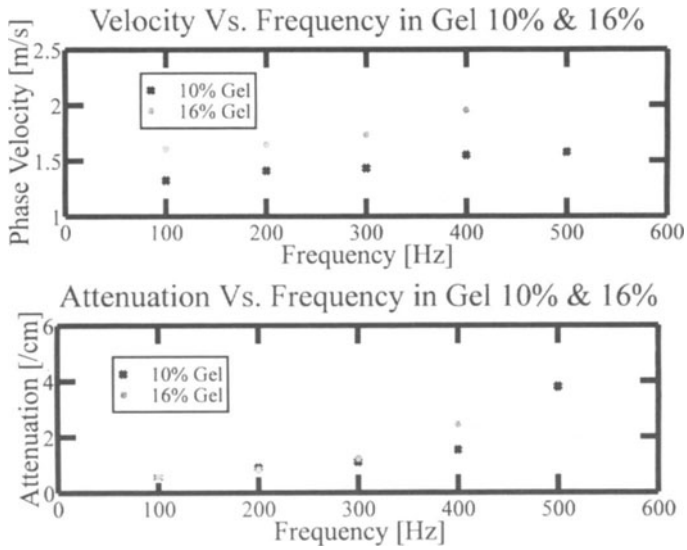

Figure 4. Dispersion plots for Gels with different composition.

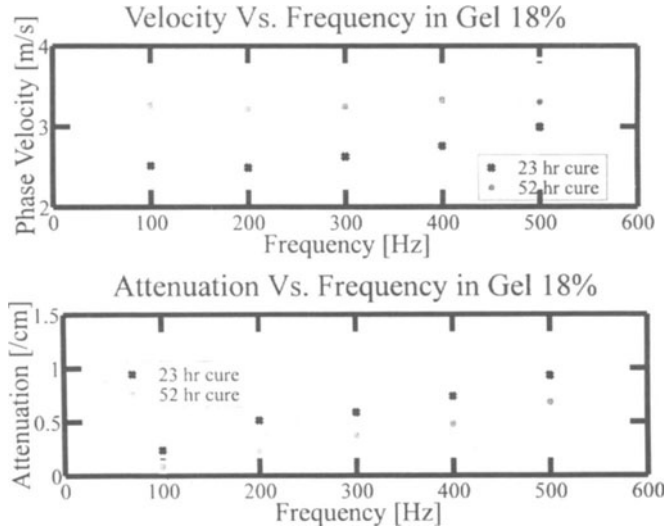

Figure 5. Dispersion plots for Gels with different cure times.

REFERENCES

1. A. Sarvazyan., "Shear Acoustic Properties of Soft Biological Tissues in Medical Diagnostics," J. Acoust. Soc. Am. Vol. 93, 2329 (1993).
2. A. Sarvazyan, et al., "Elasticity Imaging as a New Modality of Medical Imaging for Cancer Detection," Proc. Int. Workshop on Interact. Ultrasound with Biol. Media, Valenciennes, France, Vol. 1, 68-81 (1994).
3. Y. C. Fung, *Biomechanics: Mechanical Properties of Living Tissues* (Springer-Verlag, New York, 1981), pp. 35-38.
4. J. Ophir, I. Cespedes, H. Ponnekanti, Y. Yazdi, and X. Li, "Elastography: A Quantitative Method for Imaging the Elasticity of Biological Tissues," Ultrason. Imag., vol. 13, 111-134, (1991).
5. S. F. Levinson, M. Shinagawa, T. Sato, "Sonoelastic Determination of Human Skeletal Muscle Elasticity," J. Biomechanics, Vol. 28(10), 1145-1154 (1995).
6. K. J. Parker, R. M. Lerner, "Sonoelasticity of Organs: Shear Waves Ring a Bell," J. Ultrasound Med., Vol. 11, 387-392 (1992).
7. R. Muthupillai, D. J. Lomas, P. J. Rossman, J. F. Greenleaf, A. Manduca, R. L. Ehman, "Magnetic Resonance Elastography by Direct Visualization of Acoustic Strain Waves," Science, Vol. 269, 1854-1857 (1995).
8. R. Muthupillai, P. J. Rossman, D. J. Lomas, J. F. Greenleaf, S. J. Riederer, R. L. Ehman, "Magnetic Resonance Imaging by of Transverse Acoustic Strain Waves," MRM, Vol. 36, 266-274 (1996).
9. P.S. Allen, "Some Fundamental Principles of Nuclear Magnetic Resonance," in *The Physics of MRI: 1992 AAPM Summer School Proceedings*, eds. M. J. Bronskill and P. Sprawls (American Institute of Physics, Inc., Woodburry, NY, 1993), pp. 15-31.
10. Y. Yamakoshi, J. Sato and T. Sato, "Ultrasonic Imaging of Internal Vibration of Soft Tissue under forced Vibration," IEEE Trans. on Sonics Ultrason., Vol. 37(2), 45-53 (1990).
11. H. Kolsky, *Stress Waves in Solids* (Dover, New York, 1963), Chapter 5.